Supporting information for

A high-resolution unified observational data product of mesoscale convective systems and isolated deep convection in the United States for 2004 – 2017

Jianfeng Li[1*], Zhe Feng[1], Yun Qian[1*], L. Ruby Leung[1]

[1] Atmospheric Sciences and Global Change Division, Pacific Northwest National Laboratory, Richland, Washington

* *Correspondence to* Jianfeng Li (jianfeng.li@pnnl.gov) and Yun Qian (yun.qian@pnnl.gov)

Table captions

Table S1. Summary of source datasets used to develop the MCS/IDC data product

Table S2. The classification criteria of the Storm Labeling in Three Dimensions (SL3D) algorithm in this study

Table S3. Annual mean precipitation amounts and intensities for different types of precipitation in different regions of the US for 2004 – 2017

Table S4. Annual mean seasonal precipitation amounts and intensities for different types of precipitation in different regions of the US for 2004 – 2017

Table S5. Annual and seasonal mean characteristics of MCS and IDC events in the data product domain for 2004 – 2017 by using the new MCS definition

Table S6. Annual mean precipitation amounts and intensities for different types of precipitation in different regions of the US for 2004 – 2017 by using the new MCS definition

Table S7. Annual mean seasonal precipitation amounts and intensities for different types of precipitation in different regions of the US for 2004 – 2017 by using the new MCS definition

Figure captions

Figure S1. Schematic of the FLEXTRKR algorithm.

Figure S2. Schematic of CCS merging and splitting.

Figure S3. An example of CCS merging and splitting from 2005-05-07T4:00:00Z – T9:00:00Z. Cloud 1 and Cloud 2 at 5:00:00Z merged into Cloud 1 at 6:00:00Z. And Cloud 1 at 7:00:00Z at least split to Cloud 1 and Cloud 3 at 8:00:00Z.

Figure S4. Schematic of "merge" tracks and "split" tracks.

Figure S5. Definition of MCSs and IDC.

Figure S6. Seasonal cumulative distribution functions (CDFs) of PF-based lifetimes for (a) MCSs and (b) IDC in the data product domain for 2004 – 2017. Red lines denote spring, blue lines denote summer, green lines denote autumn, and black lines denote winter.

Figure S7. Annual mean monthly diurnal cycles of initiated MCS (left panel) and IDC (right panel) numbers in the data product domain for 2004 – 2017. Here, we define that an MCS or IDC event initiates when the first PF appears. Therefore, we can derive the initiated time of all MCS and IDC events, which is the basis of this figure. For example, on average, more than 7 MCSs initiated at 14:00 Local Time (LT) every June between 2004 and 2017.

Figure S8. Distributions of the fractions of different types of precipitation in each season. Here, precipitation refers to annual mean seasonal amounts for 2004 – 2017. We exclude hourly data with precipitation ≤ 1 mm h^{-1} in the calculation. The first row is for total precipitation, the second for MCS precipitation, the third for IDC precipitation, and the fourth for stratiform precipitation. The first column shows spring precipitation, the second for summer, the third for autumn, and the fourth for winter.

Figure S9. Distributions of annual mean seasonal precipitation intensities for different types of precipitation for 2004 – 2017. The first row is for total precipitation, the second for MCS precipitation, the third for IDC precipitation, and the fourth for stratiform precipitation. The first column shows spring precipitation, the second for summer, the third for autumn, and the fourth for winter. We exclude hourly data with precipitation $\leq$ 1 mm h^{-1} in the calculation.

Figure S10. Monthly mean diurnal cycles of precipitation intensities for MCSs (a, d, g, j), IDC (b, e, h, k), and stratiform (c, f, i, l) in the NGP (a, b, c), SGP (d, e, f), SE (g, h, i), and NE (j, k, l) during 2004 – 2017.

Figure S11. An example of Stage IV erroneous precipitation. Stage IV shows a large area of intense precipitation suddenly appearing at 2011-05-02T12:00:00Z, which then unexpectedly disappears at 13:00:00Z, comes back abruptly at 14:00:00Z, and finally goes away immediately at 17:00:00Z.

Figure S12. Distribution of the fraction of valid Stage IV precipitation data for 2004 – 2017. Here, "valid" means that precipitation data are available and reasonable. The erroneous precipitation discussed in the main manuscript is unreasonable and invalid.

Figure S13. Distributions of the fractions of available radar reflectivity data for 2004 – 2017 at different vertical levels. As long as radars scan a grid cell, we think it as "available" even though there is no echo.

Table S1. Summary of source datasets used to develop the MCS/IDC data product

Dataset name	NCEP/CPP L3 half-hourly 4 km Global Merged IR	Three-dimensional Gridded NEXRAD Radar (Gridrad)	NCEP Stage IV precipitation	ERA5 melting level
Dataset version	V 1	V 3.1	V 1.0	
DOI	10.5067/P4HZB9N27EKU	10.5065/D6NK3CR7	10.5065/D69Z93M3	10.24381/cds.adbb2d47
URL	https://disc.gsfc.nasa.gov/datasets/GPM_MERGIR_1/summary	https://rda.ucar.edu/datasets/ds841.0/	https://rda.ucar.edu/datasets/ds507.5/	https://cds.climate.copernicus.eu/cdsapp#!/dataset/reanalysis-era5-single-levels?tab=overview
Last access	Dec 28, 2019	Jan 2, 2020	Dec 28, 2019	Jan 24, 2020
Initial spatial resolution	Horizontal: ~ 4 km	Horizontal: 0.02° Vertical: 1 km	Horizontal: ~ 4 km	Horizontal: 0.25°
Initial temporal resolution	0.5 hours	1 hour	1 hour	1 hour

Table S2. The classification criteria of the Storm Labeling in Three Dimensions (SL3D) algorithm in this study

SL3D category	Criteria
convective	Z_H[1] = 25 dBZ echo-top height ≥ 10 km; or Z_H ≥ 45 dBZ above (Z_{melt}[2] + 1) km; or Z_H peakedness[3] exceeding thresholds[4] in at least 30% of the echo column between surface and 9 km. After the above filtering, exclude isolated convective grid points. Finally, grid points that have Z_{Hmax}[5] ≥ 25 dBZ and are immediately adjacent to other convective grid points are classified as convective.
precipitating stratiform	Z_H ≥ 20 dBZ at 3 km; or Z_H ≥ 10 dBZ at 1 km or 2 km
non-precipitating stratiform	no echo or Z_H < 20 dBZ at 3 km, and echo presents above 3 km. If no echo at 3 km – 5 km, but echo presents above 5 km, classified as an anvil.
anvil	No echo at 3 km – 5 km, but echo presents above 5 km
convective updraft	convective grid points satisfy: (1) Z_{Hmax} ≥ 40 dBZ, and (2) $\frac{\partial Z_H}{\partial z} \geq 8$ dBZ km^{-1} with echoes in at least six of eight horizontally adjacent grid volumes presents between the surface and 7 km.

[1] Z_H: logarithmic radar reflectivity.
[2] Z_{melt}: melting level height. If temperatures at different vertical levels within a grid column are all below zero, there is no melting level. In this situation, we set Z_{melt} = -2.
[3] Peakedness is the difference between the Z_H of the grid point being evaluated and the median Z_H of a horizontal 12-km radius around the point.
[4] $threshold = \max\left(4.0\,dBZ, 10.0 - \frac{Z_H^2}{337.5}\,dBZ\right)$.
[5] Z_{Hmax} denotes column max reflectivity.

Table S3. Annual mean precipitation amounts and intensities for different types of precipitation in different regions of the US for 2004 – 2017

	Precipitation amount / mm				Precipitation intensity / mm h^{-1}			
	Total	MCS	IDC	Stratiform	Total	MCS	IDC	Stratiform
NGP	515	254	116	145	3.3	4.3	3.3	2.4
SGP	613	308	149	156	4.1	5.2	4.4	2.9
SE	1,156	526	303	327	4.5	5.2	5.3	3.3
NE	889	324	228	337	3.2	3.7	3.6	2.6

Table S4. Annual mean seasonal precipitation amounts and intensities for different types of precipitation in different regions of the US for 2004 – 2017

		Precipitation amount / mm				Precipitation intensity / mm h^{-1}			
		Total	MCS	IDC	Stratiform	Total	MCS	IDC	Stratiform
NGP	spring	150	78	31	40	2.9	3.6	2.8	2.2
	summer	214	117	47	50	4.2	5.0	4.5	3.0
	autumn	109	43	27	39	2.9	3.9	3.1	2.3
	winter	42	15	11	15	1.9	2.4	1.9	1.7
SGP	spring	176	119	27	30	4.2	5.2	3.9	2.9
	summer	200	83	71	47	4.7	5.5	5.3	3.2
	autumn	150	62	36	52	4.1	5.3	4.6	3.0
	winter	87	44	16	27	2.8	3.6	2.6	2.2
SE	spring	275	157	52	66	4.6	5.3	4.8	3.3
	summer	367	112	156	99	5.2	5.7	6.1	3.7
	autumn	249	109	55	85	4.6	5.4	5.5	3.5
	winter	265	147	40	78	3.8	4.7	3.7	2.8
NE	spring	230	97	56	78	2.9	3.5	3.2	2.4
	summer	276	80	85	111	4.2	4.9	5.0	3.3
	autumn	218	75	49	94	3.2	3.8	3.6	2.6
	winter	165	72	39	55	2.4	2.9	2.4	2.1

Table S5. Annual and seasonal mean characteristics of MCS and IDC events in the data product domain for 2004 – 2017 by using the new MCS definition[1]

	MCS					IDC				
	annual	spring	summer	autumn	winter	annual	spring	summer	autumn	winter
CCS-based lifetime / hour	17.1	17.6	16.0	18.2	20.0	2.0	2.1	2.0	2.0	2.6
CCS area / km^2	135,541	172,517	93,828	139,837	295,931	6,657	9,379	4,314	6,352	21,484
CCS major axis length / km	579	667	475	615	935	99	117	85	99	173
PF-based lifetime / hour	15.0	15.6	14.1	15.8	17.1	1.6	1.6	1.6	1.6	1.8
Major axis length of the largest PF / km	321	357	264	357	518	63	69	55	68	93
PF convective area / km^2	6,119	6,468	6,091	5,897	5,697	477	496	463	487	520
PF stratiform area / km^2	28,570	34,718	17,997	34,607	67,902	1,205	1,559	774	1,517	3,113
PF mean convective rain rate / mm h^{-1}	4.5	4.0	4.8	4.6	3.9	4.1	3.4	4.5	4.3	3.0
PF mean stratiform rain rate /mm h^{-1}	2.7	2.4	2.8	2.7	2.3	2.8	2.5	3.0	2.9	2.3
Area with $Z_{Hmax} \geq 45$ dBZ within the largest PF / km^2	791	862	850	617	563	54	56	57	47	42
PF mean convective 20-dBZ echo-top height / km	6.6	6.2	7.2	6.1	5.0	6.5	6.1	7.0	6.2	5.0
Area of the largest CCF / km^2	2,094	2,081	2,317	1,754	1,392	339	355	333	337	347
Major axis length of the largest CCF / km	95	96	99	88	82	29	30	28	29	30
Max 30-dBZ echo-top height of the largest CCF / km	12.7	12.2	13.9	11.6	9.4	7.0	6.4	7.6	6.5	5.0
Max 40-dBZ echo-top height of the largest CCF / km	10.4	10.2	11.4	8.9	7.1	5.4	5.0	5.9	5.0	3.7

[1] Refer to Section 4.4 in the main manuscript for the new MCS definition.

Table S6. Annual mean precipitation amounts and intensities for different types of precipitation in different regions of the US for 2004 – 2017 by using the new MCS definition

	Precipitation amount / mm				Precipitation intensity / mm h^{-1}			
	Total	MCS	IDC	Stratiform	Total	MCS	IDC	Stratiform
NGP	515	280	89	145	3.3	4.2	3.2	2.4
SGP	613	344	113	156	4.1	5.1	4.4	2.9
SE	1,156	602	227	327	4.5	5.3	5.3	3.3
NE	889	371	181	337	3.2	3.7	3.5	2.6

Table S7. Annual mean seasonal precipitation amounts and intensities for different types of precipitation in different regions of the US for 2004 – 2017 by using the new MCS definition

		Precipitation amount / mm				Precipitation intensity / mm h^{-1}			
		Total	MCS	IDC	Stratiform	Total	MCS	IDC	Stratiform
NGP	spring	150	83	26	41	2.9	3.5	2.8	2.2
	summer	214	130	34	50	4.2	5.0	4.5	3.0
	autumn	109	50	20	39	2.9	3.8	3.0	2.3
	winter	42	17	9	16	1.9	2.4	1.9	1.7
SGP	spring	176	126	20	30	4.2	5.0	3.9	2.9
	summer	200	102	51	47	4.7	5.5	5.2	3.2
	autumn	150	70	28	52	4.1	5.2	4.5	3.0
	winter	87	47	13	27	2.8	3.5	2.6	2.2
SE	spring	275	170	39	66	4.6	5.2	4.8	3.3
	summer	367	153	115	99	5.2	5.8	6.1	3.7
	autumn	249	122	42	85	4.6	5.4	5.5	3.5
	winter	265	156	31	78	3.8	4.6	3.7	2.8
NE	spring	230	108	44	78	2.9	3.5	3.1	2.4
	summer	276	99	66	111	4.2	4.9	5.0	3.3
	autumn	218	85	39	94	3.2	3.8	3.5	2.6
	winter	165	79	31	55	2.4	2.9	2.3	2.1

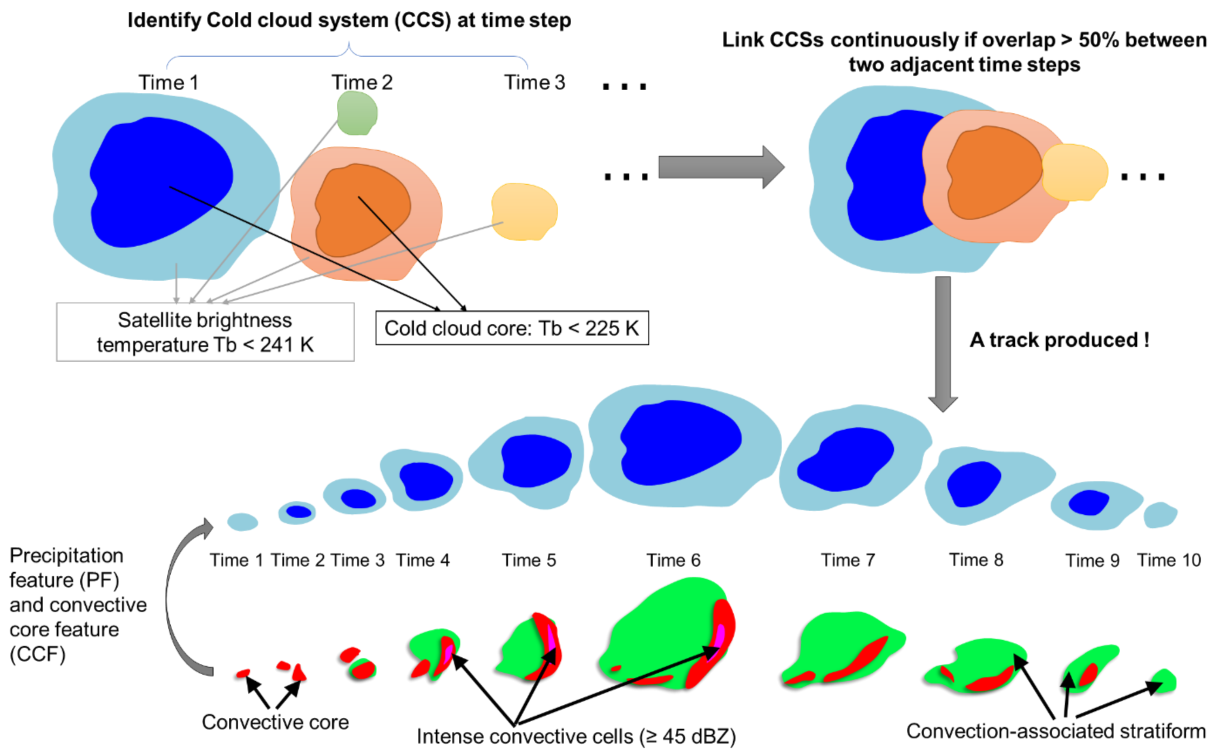

Figure S1. Schematic of the FLEXTRKR algorithm.

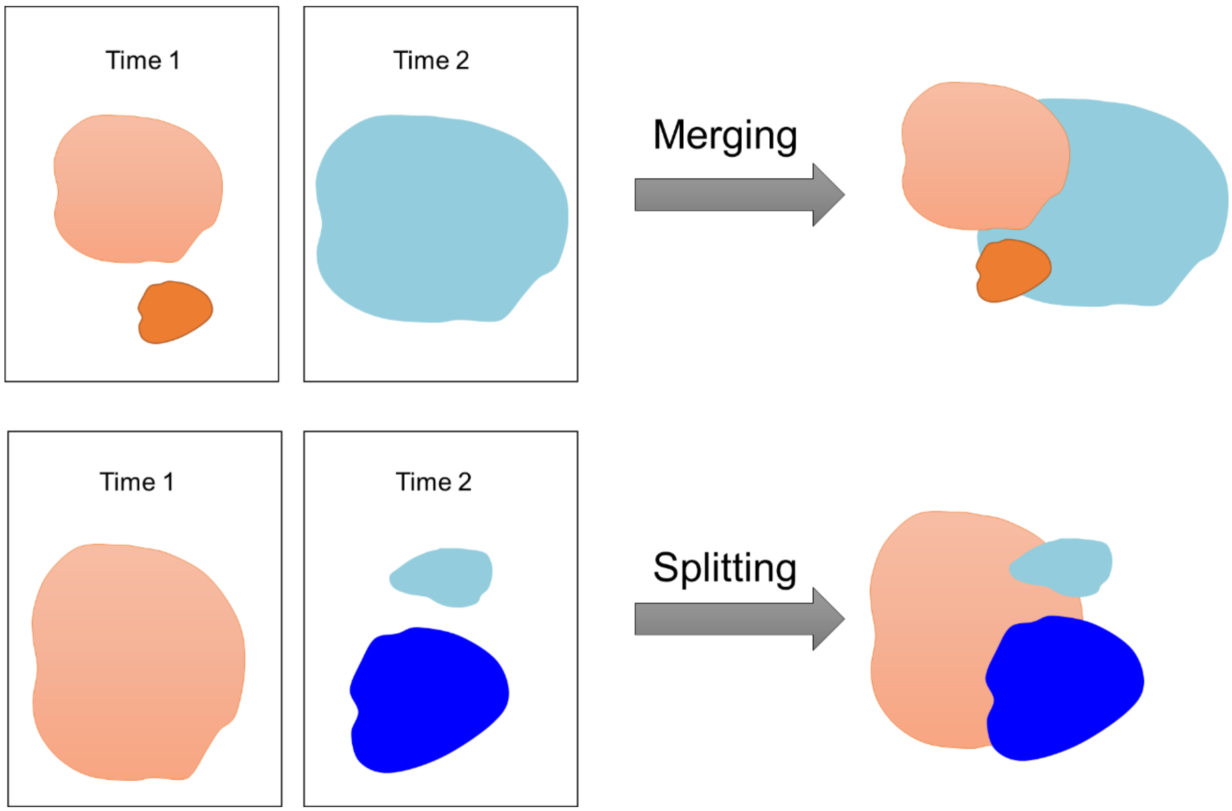

Figure S2. Schematic of CCS merging and splitting.

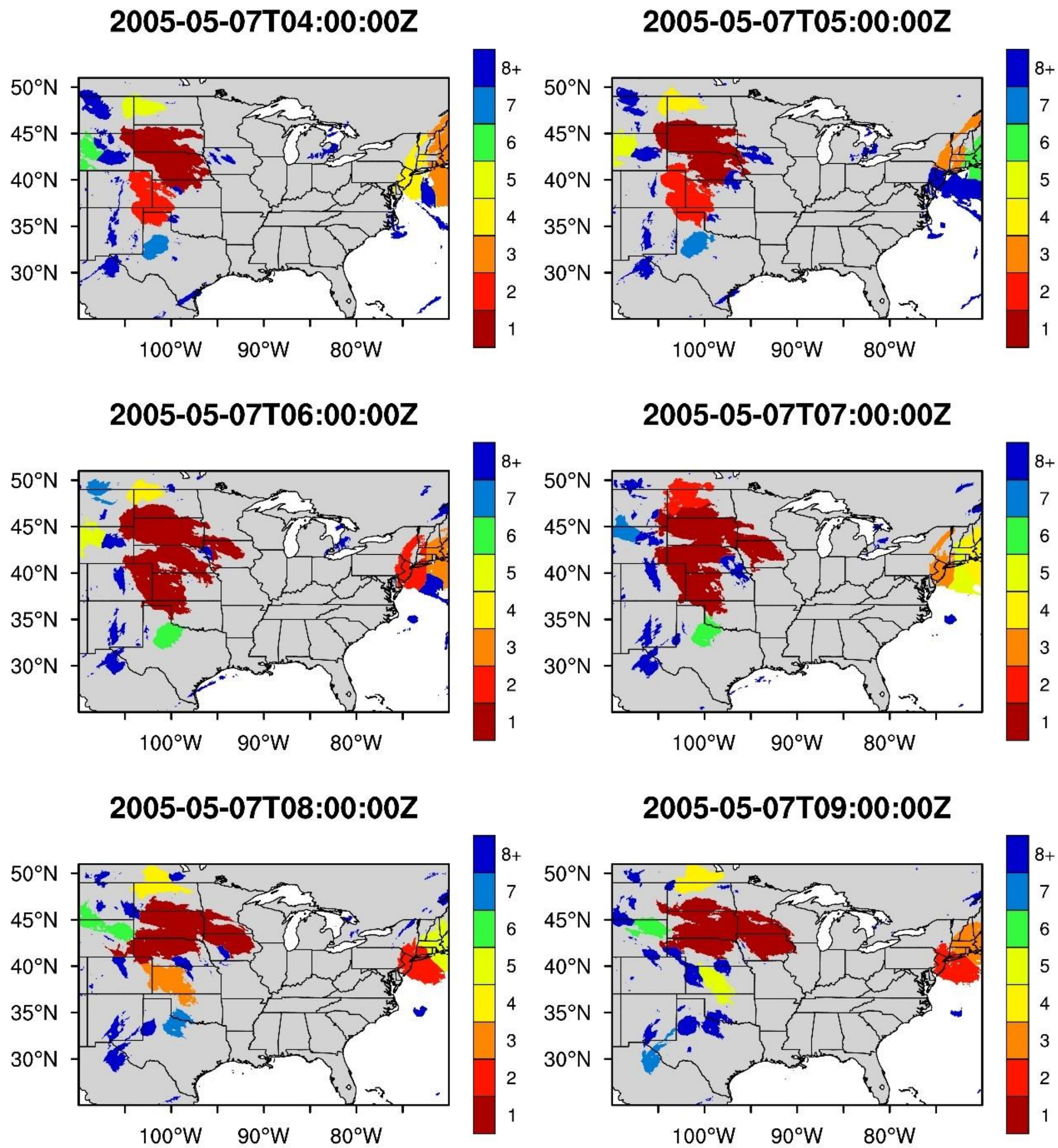

Figure S3. An example of CCS merging and splitting from 2005-05-07T4:00:00Z – T9:00:00Z. Cloud 1 and Cloud 2 at 5:00:00Z merged into Cloud 1 at 6:00:00Z. And Cloud 1 at 7:00:00Z at least split to Cloud 1 and Cloud 3 at 8:00:00Z.

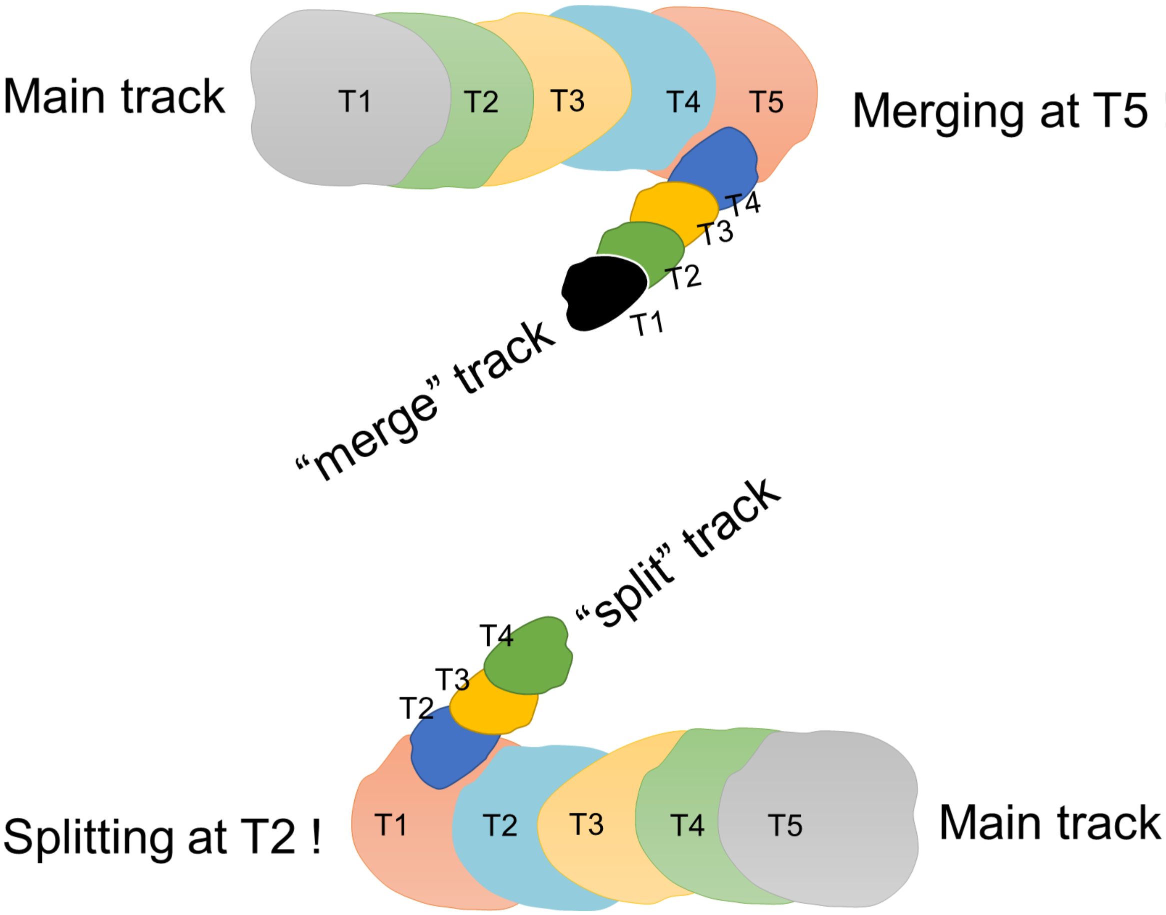

Figure S4. Schematic of “merge” tracks and “split” tracks.

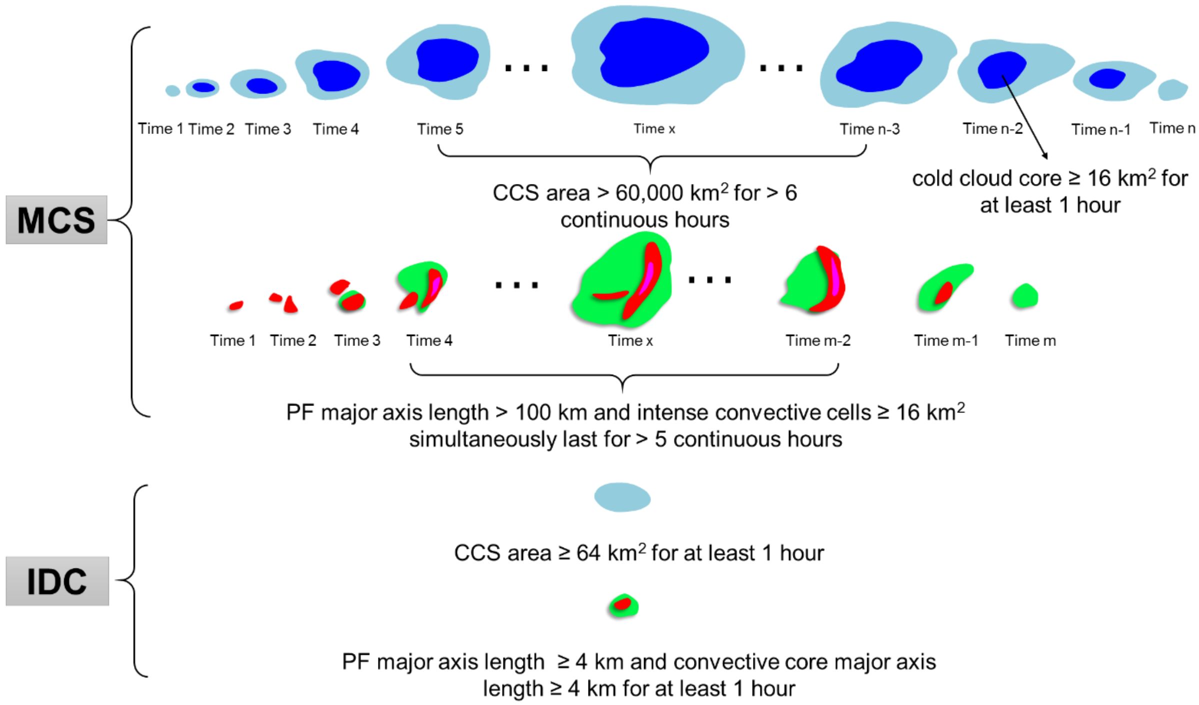

Figure S5. Definition of MCSs and IDC.

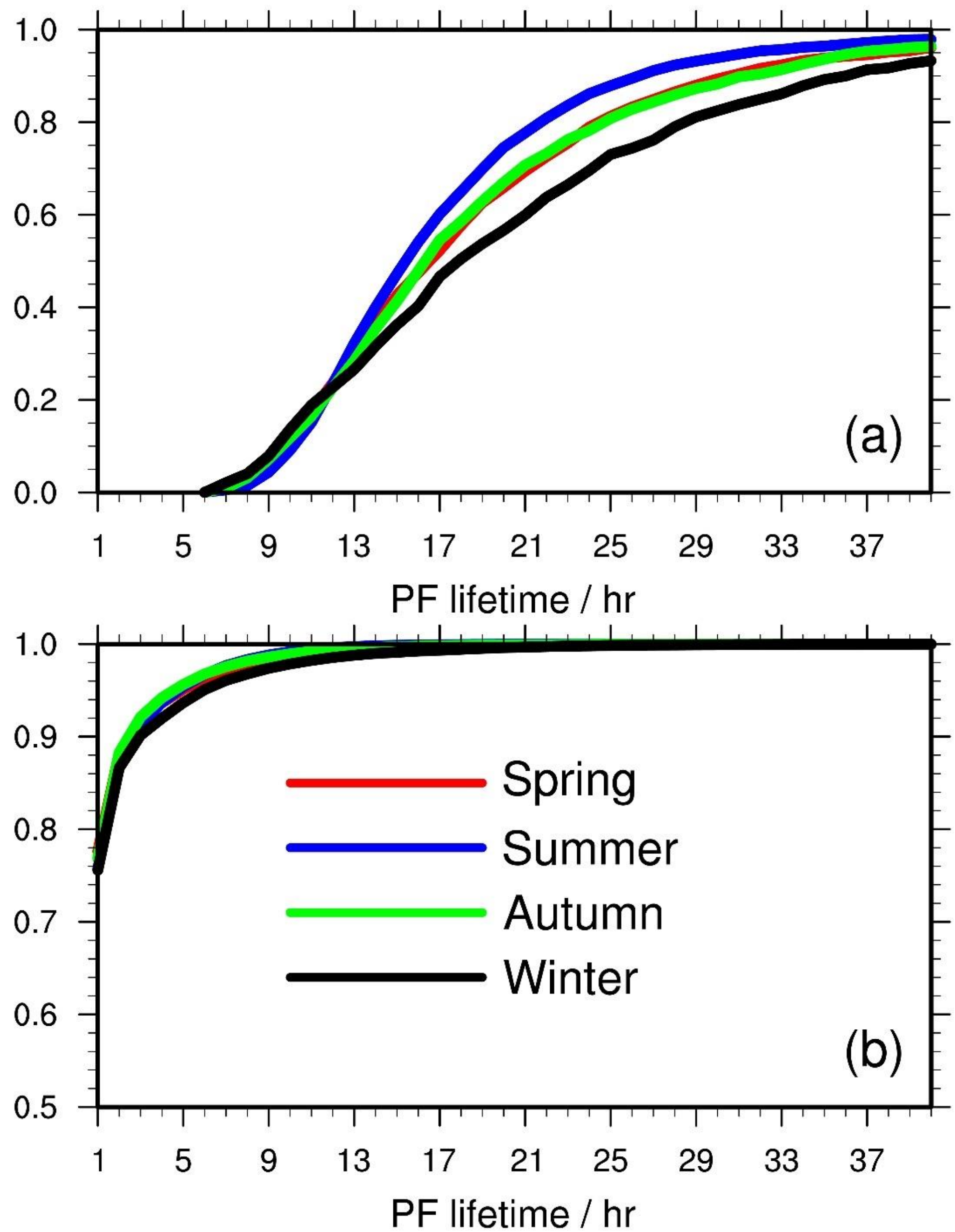

Figure S6. Seasonal cumulative distribution functions (CDFs) of PF-based lifetimes for (a) MCSs and (b) IDC in the data product domain for 2004 – 2017. Red lines denote spring, blue lines denote summer, green lines denote autumn, and black lines denote winter.

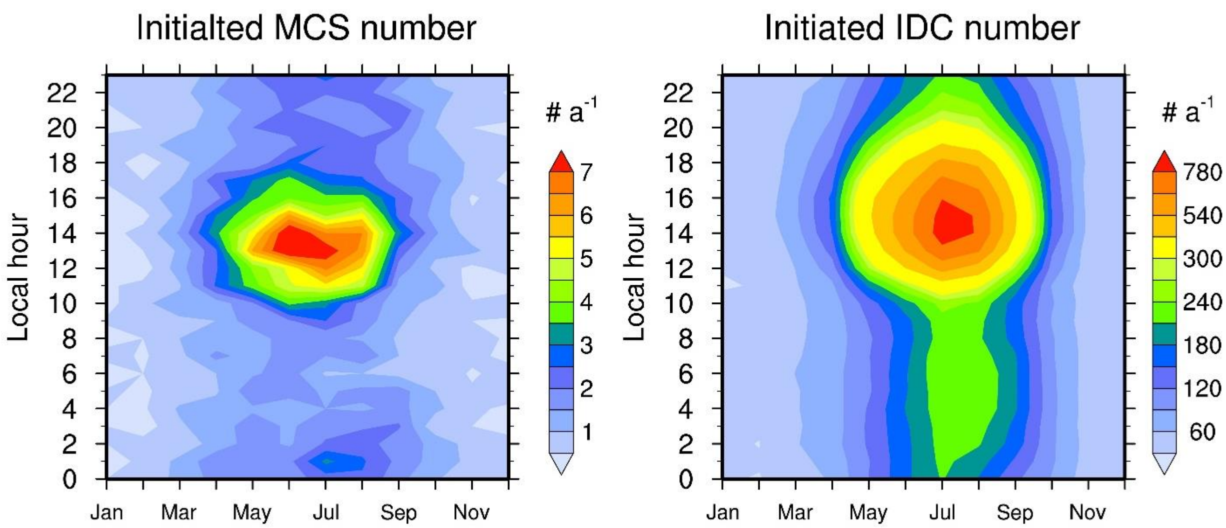

Figure S7. Annual mean monthly diurnal cycles of initiated MCS (left panel) and IDC (right panel) numbers in the data product domain for 2004 – 2017. Here, we define that an MCS or IDC event initiates when the first PF appears. Therefore, we can derive the initiated time of all MCS and IDC events, which is the basis of this figure. For example, on average, more than 7 MCSs initiated at 14:00 Local Time (LT) every June between 2004 and 2017.

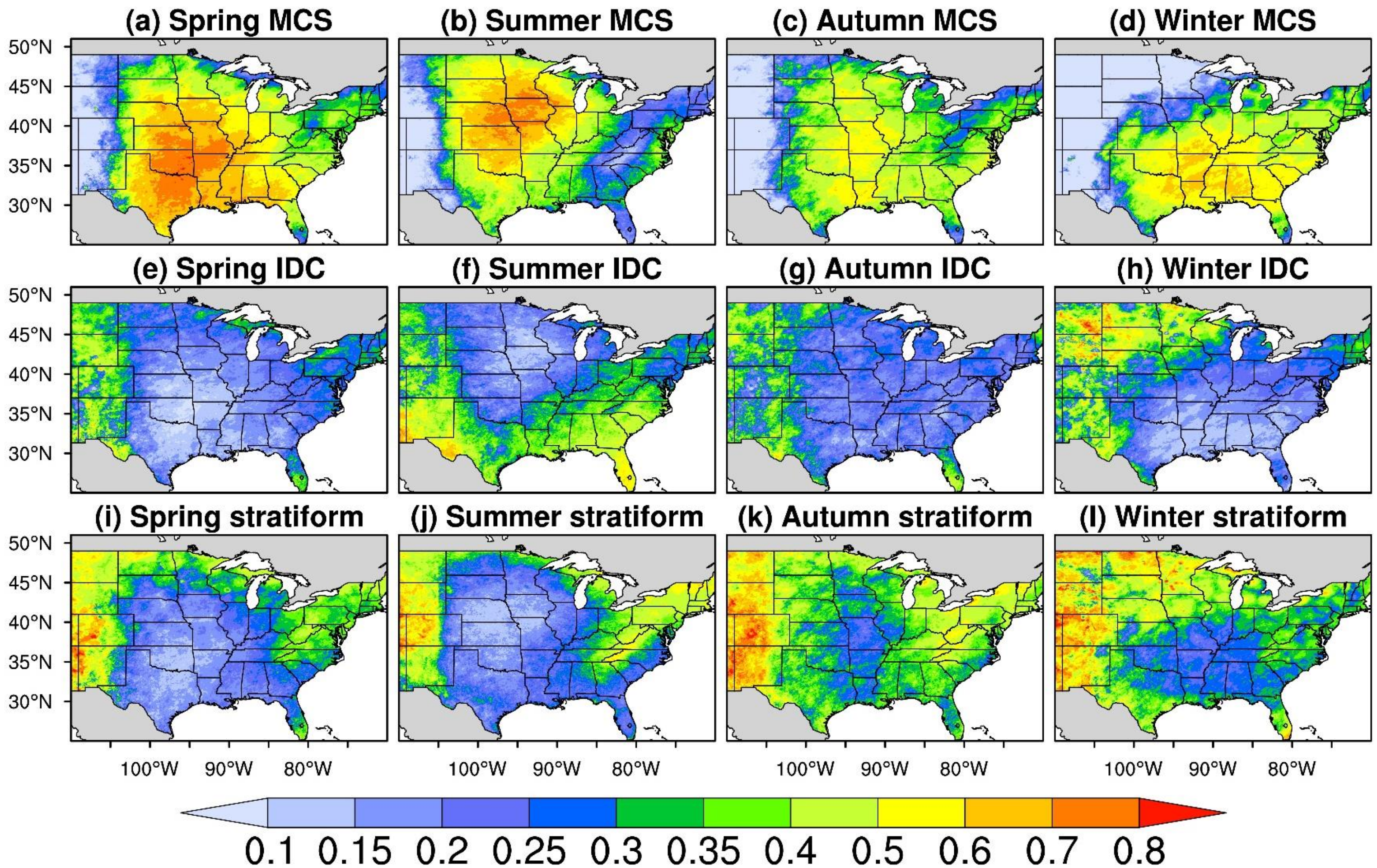

Figure S8. Distributions of the fractions of different types of precipitation in each season. Here, precipitation refers to annual mean seasonal amounts for 2004 – 2017. We exclude hourly data with precipitation $\leq$ 1 mm h^{-1} in the calculation. The first row is for total precipitation, the second for MCS precipitation, the third for IDC precipitation, and the fourth for stratiform precipitation. The first column shows spring precipitation, the second for summer, the third for autumn, and the fourth for winter.

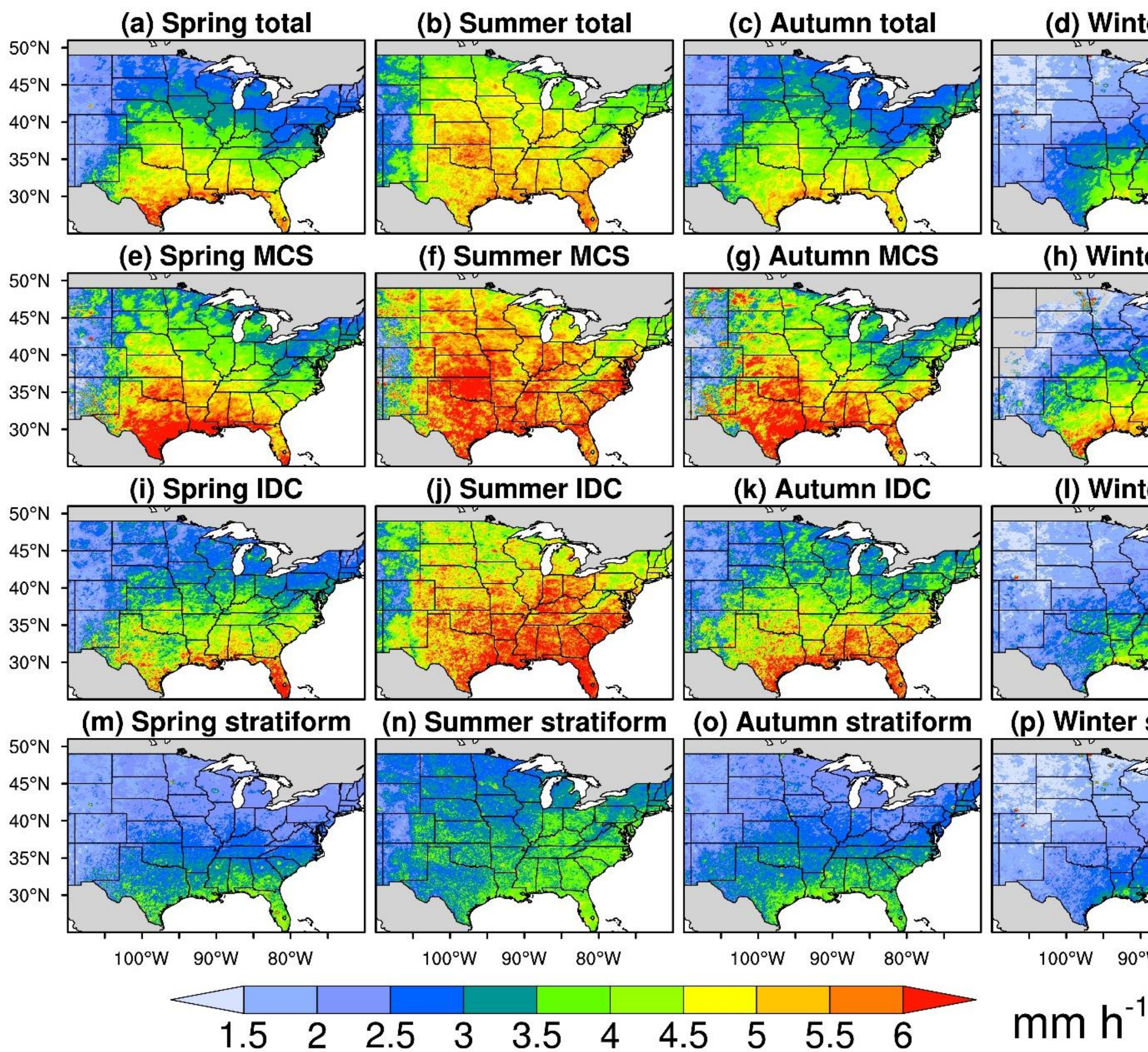

Figure S9. Distributions of annual mean seasonal precipitation intensities for different types of precipitation for 2004 – 2017. The first row is for total precipitation, the second for MCS precipitation, the third for IDC precipitation, and the fourth for stratiform precipitation. The first column shows spring precipitation, the second for summer, the third for autumn, and the fourth for winter. We exclude hourly data with precipitation ≤ 1 mm h^{-1} in the calculation.

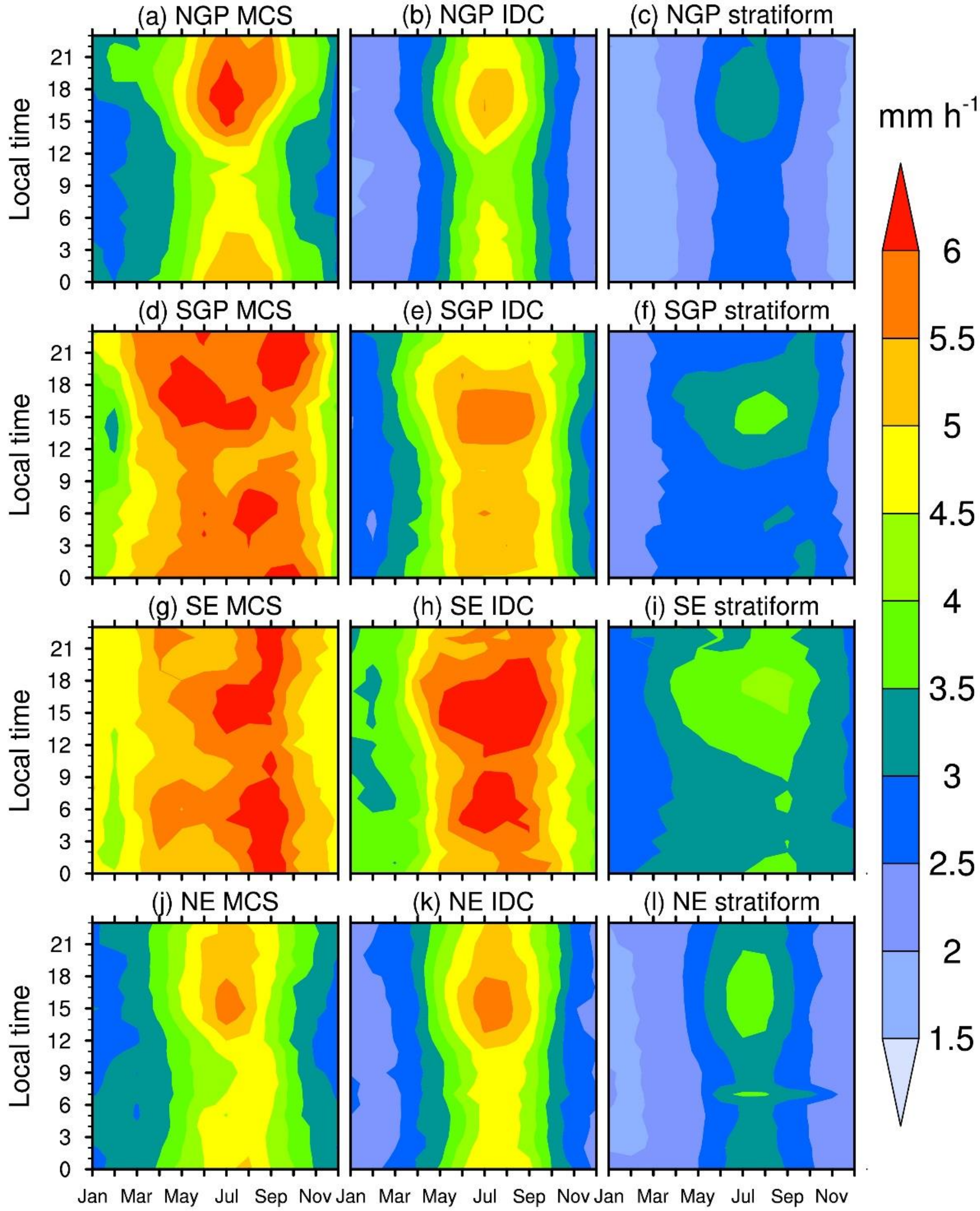

Figure S10. Monthly mean diurnal cycles of precipitation intensities for MCSs (a, d, g, j), IDC (b, e, h, k), and stratiform (c, f, i, l) in the NGP (a, b, c), SGP (d, e, f), SE (g, h, i), and NE (j, k, l) during 2004 – 2017.

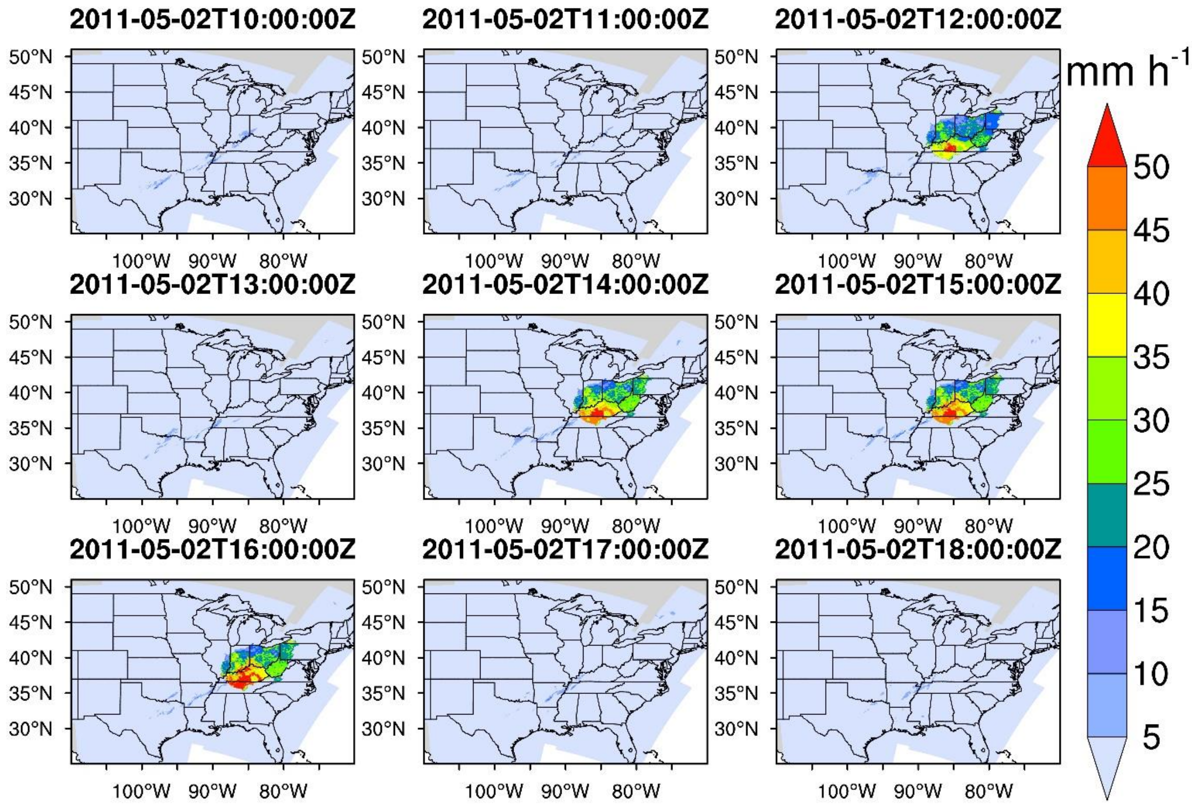

Figure S11. An example of Stage IV erroneous precipitation. Stage IV shows a large area of intense precipitation suddenly appearing at 2011-05-02T12:00:00Z, which then unexpectedly disappears at 13:00:00Z, comes back abruptly at 14:00:00Z, and finally goes away immediately at 17:00:00Z.

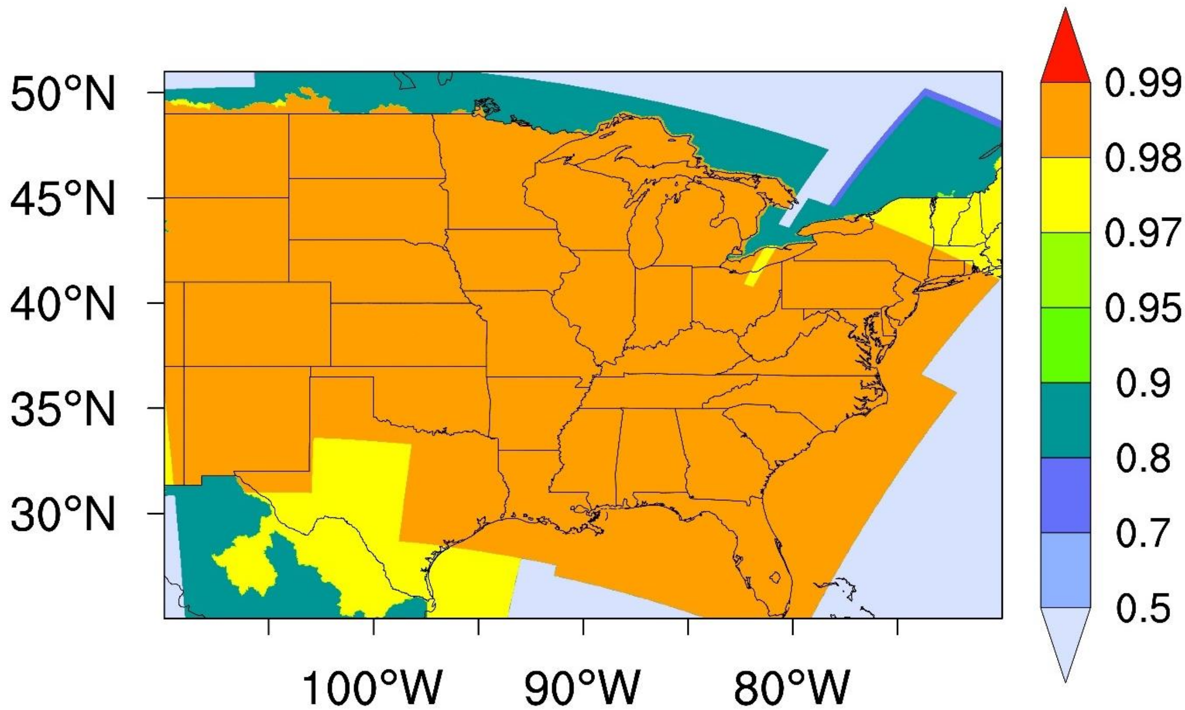

Figure S12. Distribution of the fraction of valid Stage IV precipitation data for 2004 – 2017. Here, "valid" means that precipitation data are available and reasonable. The erroneous precipitation discussed in the main manuscript is unreasonable and invalid.

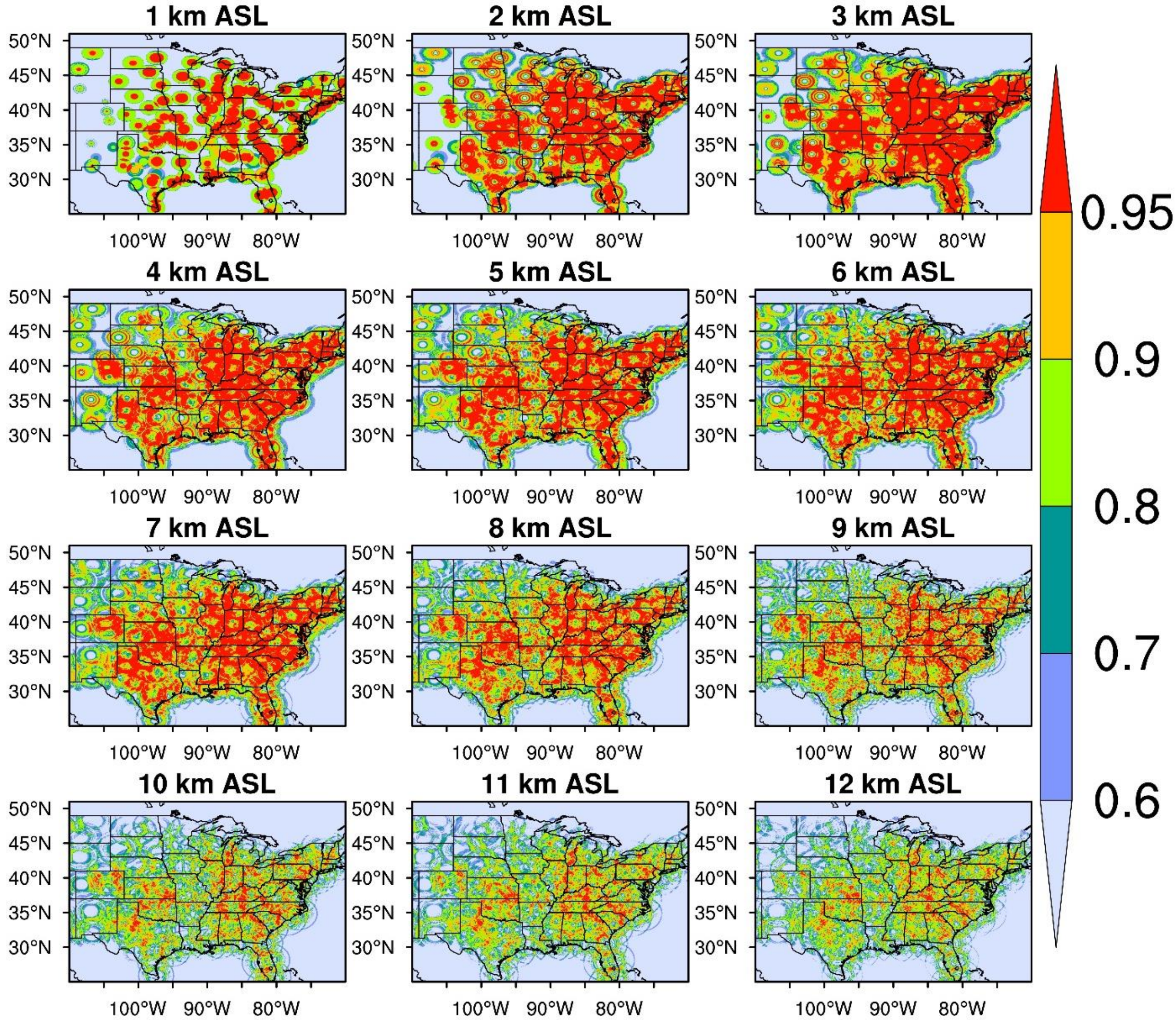

Figure S13. Distributions of the fractions of available radar reflectivity data for 2004 – 2017 at different vertical levels. As long as radars scan a grid cell, we think it as "available" even though there is no echo.